mathematics

Article

A Two-Frequency Response-Fitted Numerov-Type Scheme for Periodically Forced Oscillatory Problems

Houssem Jerbi[1], Wassim Zouch[2], Mohamed Zarouan[3], Lotfi Ladhar[4] and Theodore E. Simos[5]

1 Department of Industrial Engineering, College of Engineering, University of Hail, Hail 81481, Saudi Arabia; h.jerbi@uoh.edu.sa
2 Electrical and Computer Engineering Department, Faculty of Engineering, King Abdulaziz University, Jeddah, Saudi Arabia; wzouch@kau.edu.sa
3 Electrical and Computer Engineering Department, Faculty of Engineering, King Abdulaziz University, Jeddah, Saudi Arabia; mzarouan@kau.edu.sa
4 Department of Electrical and Computer Engineering, Faculty of Engineering, King Abdul Aziz University, Jeddah 21589, Saudi Arabia; lladhar@kau.edu.sa
5 Department of Mathematics and Natural Sciences, Gulf University for Science and Technology, West Mishref 32093, Kuwait;simos@ulstu.ru;tsimos.conf@gmail.com

Abstract: In this paper, we develop an explicit Numerov-type method for second-order initial value problems with oscillating solutions and periodic forcing. The construction takes into account two different frequencies: the frequency λ of the homogeneous oscillation and the frequency ω of the external excitation. More specifically, the coefficients are determined from $y'' = -\lambda^2 y + \exp(i\omega x)$ by requiring the numerical difference equation to reproduce both the homogeneous grid modes and the discrete forced response. Closed formulae are obtained in terms of $H = \lambda h$ and $W = \omega h$. The cases $W \to H$ and $H, W \to 0$ are examined separately in order to obtain stable expressions and the classical Numerov limit. We also study the periodicity and dissipation properties and derive the local truncation error. Finally, the efficiency of the proposed method is studied on two scalar problems and six systems of eight or ten second-order equations. Comparisons are made with classical Numerov, Dormand–Prince, Fehlberg and Chawla–Rao formulae.

Keywords: oscillatory initial value problems; Numerov-type methods; phase fitting; response fitting; periodic forcing; interval of periodicity; amplification error; second-order differential equations

MSC: 65L05; 65L06

Citation: To be assigned by the journal after publication.

Academic Editor: To be assigned

Received: –
Revised: –
Accepted: –
Published: –

Copyright: © 2026 by the author. Submission manuscript.

License information will be inserted by the publisher for the final published version.

1. Introduction

Second-order initial value problems with oscillating solutions appear in many applications, including celestial mechanics, molecular dynamics, structural mechanics, wave propagation and quantum-mechanical models. For these problems the algebraic order is not the only quantity which determines the efficiency of a numerical formula. A small error in the numerical frequency may accumulate over a long integration interval and finally dominate the global error. For this reason, methods in which information on the oscillatory character of the solution is introduced into the coefficients have been studied extensively.

For equations of second order, Numerov-type formulae are especially convenient for this purpose. Phase-fitted, amplification-fitted, exponentially fitted and trigonometrically fitted variants have been proposed, together with fitted Runge–Kutta–Nyström and hybrid methods. Their common feature is that available information on the principal frequency is used during the construction of the method.

A periodically forced oscillator requires one additional consideration. When the natural frequency is λ and the forcing frequency is ω, the exact solution contains a homogeneous component associated with λ and a particular component associated with ω. Exact treatment of the homogeneous phase does not in general imply exact treatment of the forced response. Consequently, the two quantities have to be included separately in the fitting conditions.

Taking into account the above observation, we introduce the two independent parameters $H = \lambda h$ and $W = \omega h$. The coefficients of the explicit Numerov-type predictor–corrector considered below are calculated from the complete difference equation of a periodically forced test problem. In this way the natural grid modes and the inhomogeneous grid response are fitted simultaneously.

The general ideas of phase fitting, response fitting and two-frequency fitting are already present in the literature. The contribution considered here is the construction obtained for the particular explicit predictor–corrector: the coefficient system, its closed solution, the continuation for $W = H$, the stability and local-error analysis, and the numerical study on scalar and vector problems.

The paper is developed as follows. In Section 2 we present the numerical formula and the fitting equation. In Section 3 we derive the exact and numerical difference equations and calculate the coefficients. The limiting cases are considered in Section 4. The stability analysis and the local truncation error are given in Sections 5 and 6, respectively. Section 7 contains the implementation details. The numerical results are presented in Section 8. Finally, Sections 9 and 10 contain the discussion and conclusions.

1.1. Relation with earlier fitted integrators

Periodically forced second-order equations and fitted Numerov-type formulae have been considered by several authors. Earlier work on periodic forcing, phase-fitted Numerov methods, phase- and amplification-fitted hybrid formulae, and two-frequency methods provides the background of the present construction. These results also show why the homogeneous phase and the forced amplitude should be regarded as different numerical quantities.

Here we use the exact grid recurrence of an explicitly inhomogeneous scalar equation. The two natural grid modes and the forced grid mode are reproduced by the same three-term recurrence. Together with the Numerov normalization, these requirements give three relations for a, b_0 and b_1. Except at the discrete aliasing points discussed below, the resulting coefficient triple is uniquely determined.

To place the present construction more precisely within the existing literature, Table 1 summarizes the main lines of development that are directly related to the proposed formula. The last column is intentionally stated in a restricted form: it identifies the additional feature introduced here and should not be read as a general priority claim over all fitted integrators.

2. Numerical Formula and Fitting Model

We consider second-order initial value problems of the form

$$y'' = f(x, y), \qquad y(x_0) = y_0, \qquad y'(x_0) = v_0. \tag{1}$$

Let $x_n = x_0 + nh$ and let y_n denote the numerical approximation to $y(x_n)$. For the numerical solution of the above problem we use the following two-step predictor–corrector. The predicted value is

$$y^p_{n+1} = 2y_n - y_{n-1} + ah^2 y''_n, \tag{2}$$

and the corrected value is given by

$$y_{n+1} - 2y_n + y_{n-1} = h^2 \left[b_0 \left((y^p_{n+1})'' + y''_{n-1} \right) + b_1 y''_n \right]. \tag{3}$$

The coefficient a appears in the predictor. For $a = 1$, $b_0 = 1/12$ and $b_1 = 5/6$ the classical formula is recovered. Thus the normalization used below is $2b_0 + b_1 = 1$.

2.1. Two-frequency model

In order to determine the frequency-dependent coefficients, we apply the formula to

$$y'' = -\lambda^2 y + \exp(i\omega x), \qquad \omega \neq \lambda, \tag{4}$$

and introduce the dimensionless quantities

$$H = \lambda h, \qquad W = \omega h. \tag{5}$$

In the derivation we first assume $H \neq W$. The case $H = W$ is obtained afterwards by continuity. This avoids introducing the resonant form of the differential equation before the removable singularities of the coefficient functions have been resolved.

Table 1. Position of the present method with respect to closely related literature.

Reference	Main idea	Frequencies/response treated	Relation to the present work
van der Houwen et al. [1]	RKN and predictor–corrector methods for second-order IVPs with periodic external forcing	Accurate representation of the oscillation generated by the periodic forcing; phase-lag and dissipation conditions for the forced component	Establishes the periodically forced integration setting. The present formula instead derives one explicit Numerov-type recurrence by matching simultaneously the natural homogeneous modes and an independently specified forcing mode.
Simos and Williams [2]	Explicit Numerov-type methods with minimal phase lag for oscillatory and Schrödinger-type problems	Fitting is directed primarily at the oscillatory homogeneous solution	Provides part of the phase-fitted Numerov background. Here a second, independent forcing frequency is included explicitly in the coefficient equations.
Simos, Famelis and Tsitouras [3]; Bratsos et al. [8]	Zero-dissipative and phase-fitted Numerov-type constructions	Phase properties of oscillatory second-order IVPs	The present construction retains the Numerov framework but adds an inhomogeneous response-matching condition to the homogeneous phase condition.
Van de Vyver [5, 6]	Explicit Numerov-type and phase-/amplification-fitted two-step hybrid methods	Phase and, in the hybrid setting, amplification fitting	Closely related fitted methodology. Our coefficients are obtained from the exact grid recurrence of an explicitly forced model and include the response factor $\Phi(H, W)$.
Fang, You and Chen [7]	Phase- and amplification-fitted Numerov-type methods for periodic IVPs with two frequencies	Two-frequency fitting in a Numerov-type setting	This is the closest two-frequency antecedent. The distinction here is the explicit inhomogeneous model $y'' = -\lambda^2 y + e^{i\omega x}$ with independent $H = \lambda h$ and $W = \omega h$, and simultaneous matching of normalization, homogeneous propagation and the discrete forced-response coefficient.
Present method	Explicit predictor–corrector Numerov-type formula with a in the predictor and b_0, b_1 in the corrector	Independent natural and forcing frequencies; exact fitted grid response	Closed-form a, b_0, b_1 from the exact inhomogeneous recurrence; stable sinc representation of $\Phi(H, W)$; analytic continuation for $W \to H$; classical $H, W \to 0$ limit; frozen-coefficient stability and LTE analysis for this specific formula.

3. Exact Grid Recurrence and Determination of the Coefficients

3.1. Continuous solution and discrete forcing factor

For $\omega \neq \lambda$, a particular solution has the form $C\,exp(i\,\omega\,x)$. Substitution gives $C = (\lambda^2 - \omega^2)^(- 1)$. Therefore the exact solution is a linear combination of $\exp(i\,\lambda\,x)$, $\exp(-i\,\lambda\,x)$, and the forced component $\frac{\exp(i\,\omega\,x)}{\lambda^2-\omega^2}$. Applying the centered operator associated with the natural frequency to the exact grid values eliminates both homogeneous modes.

$$y_{n+1} - 2\cos(H)y_n + y_{n-1} = h^2\Phi(H,W)e^{i\omega x_n}, \tag{6}$$

where

$$\Phi(H,W) = \frac{2(\cos W - \cos H)}{H^2 - W^2}. \tag{7}$$

For $H \simeq W$ the last quotient should not be evaluated directly. Using the difference-of-cosines identity, we obtain

$$\Phi(H,W) = sinc((H+W)/2)sinc((H-W)/2), sinc(z) = \sin(z)/z. \tag{8}$$

This form is used for the numerical evaluation of the response factor.

3.2. Numerical recurrence

We now apply the predictor and corrector to the same fitting equation. After substitution and collection of the terms containing y_n, y_{n-1} and $\exp(i\omega x_n)$, the method is reduced to a three-term difference equation. Comparison with the exact grid relation gives the required conditions.

The first relation is the classical Numerov normalization

$$2b_0 + b_1 = 1. \tag{9}$$

The second relation is obtained by requiring exact propagation of the natural-frequency grid modes, while the third equates the numerical forcing coefficient to $\Phi(H,W)$. To solve these relations we put

$$S(H) = 2[1 - \cos(H)]/H^2 = [\sin(H/2)/(H/2)]^2. \tag{10}$$

The resulting coefficients are

$$b_0(H,W) = [S(H) - \Phi(H,W)]/[4sin^2(W/2)], \tag{11}$$

$$b_1(H,W) = 1 - 2b_0(H,W), \tag{12}$$

$$a(H,W) = [1 - S(H)]/[H^2 b_0(H,W)]. \tag{13}$$

These are the coefficients of the proposed method. We note that W enters b_0 and b_1 through the response factor, whereas the product ab_0 can be expressed only in terms of H.

Theorem 1 (Closed-form coefficients and exact fitted recurrence)**.** *Let the explicit predictor–corrector of Section 2 be applied to*

$$y'' = -\lambda^2 y + e^{i\omega x}, \qquad H = \lambda h, \quad W = \omega h,$$

and impose the normalization $2b_0 + b_1 = 1$*. Away from the discrete aliasing values* $W = 2k\pi$ *and away from points where the resulting* $b_0(H,W) = 0$*, the simultaneous requirements of exact homogeneous propagation and exact discrete forced response determine a unique finite coefficient triple. It is*

$$\boxed{\begin{aligned} b_0(H,W) &= \frac{S(H) - \Phi(H,W)}{4\sin^2(W/2)}, \\ b_1(H,W) &= 1 - 2b_0(H,W), \\ a(H,W) &= \frac{1 - S(H)}{H^2 b_0(H,W)}. \end{aligned}}$$

where

$$\boxed{\begin{aligned} S(H) &= \frac{2(1-\cos H)}{H^2}, \\ \Phi(H,W) &= \frac{2(\cos W - \cos H)}{H^2 - W^2}. \end{aligned}}$$

With these coefficients the numerical three-term recurrence coincides with

$$\boxed{y_{n+1} - 2\cos(H)y_n + y_{n-1} = h^2\Phi(H,W)e^{i\omega x_n}.}$$

Consequently the grid modes $e^{i\lambda x}$, $e^{-i\lambda x}$ and $e^{i\omega x}$ are reproduced exactly when the starting values are exact.

The proof of Theorem 1, including the two intermediate recurrences used in the matching argument, is given in Appendix A.

3.3. Uniqueness and aliasing

Away from the zeros of the denominator generated by the discrete forcing mode, and provided $b_0 \neq 0$, the three matching conditions determine a unique finite triple (a, b_0, b_1). The exceptional values W=2k pi are discrete aliasing points because the forcing has the same value at successive grid points. At such points the usual identification of the forced coefficient loses information. This is a property of the sampled forcing and not a failure of the continuous differential equation.

The three conditions are neither redundant nor arbitrary. If normalization is removed, a family of response-matched formulas remains. If the homogeneous condition is removed, the forcing can be fitted while the natural phase drifts. If the response condition is removed, the method reduces to a conventional phase-fitted construction that does not determine the particular-solution coefficient. The full system is therefore the smallest one that expresses the intended design of this predictor-corrector formula.

4. Limiting Cases and Stable Evaluation

4.1. Diagonal continuation

We next take the limit $W \to H$. Although the usual representation of the particular solution is singular at resonance, the coefficient functions have finite limits. From the sinc form of Φ we obtain

$$\Phi(H,H) = \sin(H)/H. \tag{14}$$

Consequently, on the diagonal

$$b_0(H,H) = [\sin(H/2)/(H/2)]^2 - \sin(H)/H/[4sin^2(H/2)], \tag{15}$$

$$b_1(H,H) = 1 - 2b_0(H,H), \tag{16}$$

$$a(H,H) = 1 - [\sin(H/2)/(H/2)]^2/[H^2 b_0(H,H)]. \tag{17}$$

This diagonal formula is particularly important in applications where the dominant external excitation is close to a natural frequency. It also avoids subtracting nearly equal cosines in floating-point arithmetic.

4.2. Classical limit

Taking the Taylor expansions at the origin, as $H, W \to 0$ we obtain

$$a \to 1, b_0 \to 1/12, b_1 \to 5/6. \tag{18}$$

The limiting process must be carried out after the removable quotients have been resolved. Substituting H=W=0 directly into the raw closed forms gives indeterminate expressions and is therefore unsuitable for software.

4.3. Taylor expansions of the fitted coefficients

For small values of the fitted arguments, the closed formulae should be replaced by their Taylor expansions. Since $H = \lambda h$ and $W = \omega h$, a term of total degree $2j$ in (H, W) is of order h^{2j}. The following formulae retain all terms through total degree ten; hence the omitted terms are $O(h^{12})$ for fixed λ and ω.

4.3.1. Non-diagonal case: H and W independent

For H and W treated as independent small parameters, we obtain

$$\begin{aligned} b_0(H,W) = {} & \frac{1}{12} - \frac{2H^2 - 3W^2}{720} + \frac{(H^2 - 2W^2)(3H^2 - 5W^2)}{60480} \\ & - \frac{(2H^2 - 3W^2)(H^4 - 5H^2W^2 + 7W^4)}{3628800} \\ & + \frac{(H^2 - 3W^2)(2H^6 - 14H^4W^2 + 37H^2W^4 - 30W^6)}{479001600} \\ & - \frac{30H^{10} - 425H^8W^2 + 2578H^6W^4 - 8147H^4W^6 + 12874H^2W^8 - 7601W^{10}}{1307674368000} + O(h^{12}), \end{aligned} \tag{19}$$

and, from $b_1 = 1 - 2b_0$,

$$\begin{aligned} b_1(H,W) = \frac{5}{6} &+ \frac{2H^2 - 3W^2}{360} - \frac{(H^2 - 2W^2)(3H^2 - 5W^2)}{30240} \\ &+ \frac{(2H^2 - 3W^2)(H^4 - 5H^2W^2 + 7W^4)}{1814400} \\ &- \frac{(H^2 - 3W^2)(2H^6 - 14H^4W^2 + 37H^2W^4 - 30W^6)}{239500800} \\ &+ \frac{30H^{10} - 425H^8W^2 + 2578H^6W^4 - 8147H^4W^6 + 12874H^2W^8 - 7601W^{10}}{653837184000} + O(h^{12}). \end{aligned} \tag{20}$$

The predictor coefficient is

$$\begin{aligned} a(H,W) = 1 &- \frac{W^2}{20} + \frac{13W^2(H^2 + W^2)}{25200} + \frac{W^2(2H^4 - 11H^2W^2 + 2W^4)}{504000} \\ &- \frac{W^2(H^2 + W^2)(31H^4 - 473H^2W^2 + 31W^4)}{6985440000} \\ &- \frac{W^2(2686H^8 - 20831H^6W^2 + 40516H^4W^4 - 20831H^2W^6 + 2686W^8)}{5448643200000} + O(h^{12}). \end{aligned} \tag{21}$$

Equivalently, after inserting $H = \lambda h$ and $W = \omega h$, the first terms are

$$b_0 = \frac{1}{12} + \frac{3\omega^2 - 2\lambda^2}{720}h^2 + \frac{(\lambda^2 - 2\omega^2)(3\lambda^2 - 5\omega^2)}{60480}h^4 + \cdots + O(h^{12}), \tag{22}$$

$$b_1 = \frac{5}{6} + \frac{2\lambda^2 - 3\omega^2}{360}h^2 - \frac{(\lambda^2 - 2\omega^2)(3\lambda^2 - 5\omega^2)}{30240}h^4 + \cdots + O(h^{12}), \tag{23}$$

$$a = 1 - \frac{\omega^2}{20}h^2 + \frac{13\omega^2(\lambda^2 + \omega^2)}{25200}h^4 + \cdots + O(h^{12}), \tag{24}$$

where the complete h^6, h^8 and h^{10} terms are given explicitly by (19)–(21).

4.3.2. Diagonal case: $H = W$

On the diagonal, $W = H = \lambda h$, the preceding expressions reduce to

$$b_0(H,H) = \frac{1}{12} + \frac{H^2}{720} + \frac{H^4}{30240} + \frac{H^6}{1209600} + \frac{H^8}{47900160} + \frac{691H^{10}}{1307674368000} + O(h^{12}), \tag{25}$$

$$b_1(H,H) = \frac{5}{6} - \frac{H^2}{360} - \frac{H^4}{15120} - \frac{H^6}{604800} - \frac{H^8}{23950080} - \frac{691H^{10}}{653837184000} + O(h^{12}), \tag{26}$$

$$a(H,H) = 1 - \frac{H^2}{20} + \frac{13H^4}{12600} - \frac{H^6}{72000} + \frac{137H^8}{1164240000} - \frac{2113H^{10}}{2724321600000} + O(h^{12}). \tag{27}$$

These diagonal series are obtained either by expanding the analytic continuation $\Phi(H,H) = \sin H/H$ or by setting $W = H$ in the two-parameter expansions above. The two procedures give identical coefficients through order ten and provide a useful algebraic check on the removable-resonance continuation.

Theorem 2 (Diagonal continuation, classical limit and small-step expansion)**.** *The coefficient functions of Theorem 1 possess a finite analytic continuation to $W = H$. On the diagonal,*

$$\boxed{\Phi(H,H) = \frac{\sin H}{H}}$$

and the same closed coefficient relations remain valid with this continued value. Moreover,

$$\boxed{\lim_{H,W\to 0} a = 1, \qquad \lim_{H,W\to 0} b_0 = \frac{1}{12}, \qquad \lim_{H,W\to 0} b_1 = \frac{5}{6}}$$

For fixed physical frequencies, the two-parameter and diagonal Taylor expansions displayed in this section contain all terms through total degree ten and have remainder $O(h^{12})$.

A proof of the removable diagonal limit, the classical limit, and the consistency of the diagonal and two-parameter Taylor series is given in Appendix B.

4.4. Practical coefficient evaluation

In the implementation we use the sinc product for ordinary arguments, the diagonal expression when W is close to H, and Taylor expansions near the origin. The switching tolerances depend on the working precision.

This point is essential in long integrations. A theoretically exact fitted recurrence can lose its advantage if the coefficients are evaluated by subtracting nearly equal floating-point numbers at every step. In the experiments reported below the coefficient evaluation is separated from the time-stepping loop whenever H and W are constant.

5. Stability, Periodicity and Dissipation

5.1. Frozen-coefficient homogeneous test

For the stability study, the fitted coefficients are frozen at a selected pair (H, W) and the method is applied to the homogeneous probe oscillator

$$y'' = -\mu^2 y, \qquad V = \mu h. \tag{28}$$

The predictor becomes

$$y^p_{n+1} = (2 - aV^2)y_n - y_{n-1}. \tag{29}$$

Substitution in the corrector gives

$$y_{n+1} - 2A_s(V; H, W)y_n + y_{n-1} = 0, \tag{30}$$

where

$$A_s(V; H, W) = 1 - \frac{V^2}{2}\left(2b_0 + b_1 - ab_0V^2\right). \tag{31}$$

Using the normalization $2b_0 + b_1 = 1$,

$$A_s(V; H, W) = 1 - \frac{V^2}{2} + \frac{a(H, W)b_0(H, W)}{2}V^4. \tag{32}$$

5.2. Independence from the forcing frequency

The fitted phase relation gives

$$a(H, W)b_0(H, W) = c(H) = \frac{1 - S(H)}{H^2} = \frac{H^2 - 4\sin^2(H/2)}{H^4}. \tag{33}$$

Consequently,

$$\boxed{A_s(V; H) = 1 - \frac{V^2}{2} + \frac{c(H)}{2}V^4} \tag{34}$$

and the forcing parameter W disappears from the frozen homogeneous stability function. This is an important property of the proposed response-fitted construction: W changes the individual coefficients and the inhomogeneous response, but it does not change the homogeneous periodicity boundary.

At the fitted point $V = H$,

$$A_s(H; H) = \cos H, \tag{35}$$

so the selected natural-frequency mode is propagated with its exact grid phase.

5.3. Stability set and first interval of periodicity

The characteristic equation is

$$\zeta^2 - 2A_s(V; H)\zeta + 1 = 0. \tag{36}$$

Its roots are distinct complex conjugates of unit modulus whenever

$$|A_s(V; H)| < 1. \tag{37}$$

Thus, for a frozen value of H, the periodicity set is

$$\mathcal{P}_H = \{V \geq 0 : \ |A_s(V; H)| < 1\}. \tag{38}$$

The first interval of periodicity is $(0, V_0)$, where

$$V_0(H) = \begin{cases} \left[\dfrac{1 - \sqrt{1 - 16c(H)}}{2c(H)}\right]^{1/2}, & 0 < c(H) \leq 1/16, \\ \dfrac{1}{\sqrt{c(H)}}, & c(H) > 1/16. \end{cases} \tag{39}$$

At the transition $c(H) = 1/16$, the stability function touches -1 at $V = \sqrt{8}$; hence the first open interval ends at $\sqrt{8}$, not at $1/\sqrt{c(H)} = 4$.

For the values used below,

$$\begin{aligned} V_0(1) &= 3.5222490026, \\ V_0(10) &= 2.0413902656, \\ V_0(50) &= 2.0016044519, \\ V_0(100) &= 2.0004002692. \end{aligned} \tag{40}$$

5.4. Stability diagrams for representative fitted pairs

Figures 1–3 show the stability function for the requested fitted pairs. The hatched part of each diagram denotes the set for which $|A_s| < 1$; the dotted vertical line gives the end V_0 of the first periodicity interval. The pairs $(H, W) = (1, 1)$ and $(1, 10)$ produce identical stability diagrams, and the same is true for $(10, 10)$ and $(10, 1)$. These coincidences are not numerical accidents: they are direct graphical confirmations that the frozen homogeneous stability function is independent of W.

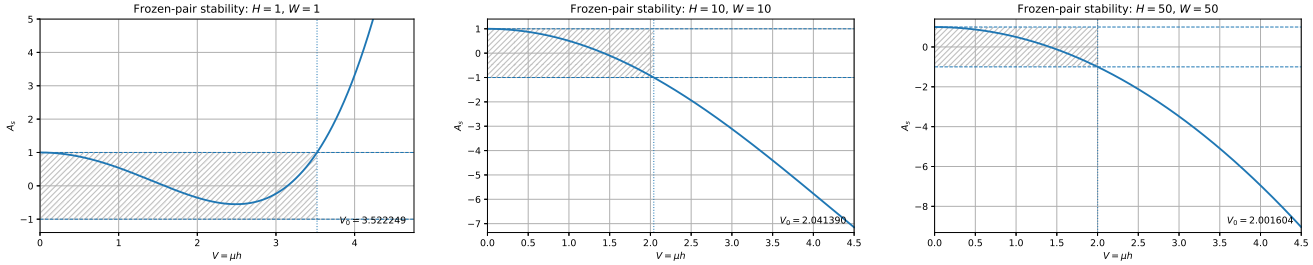

(a) $H = 1,\ W = 1$ (b) $H = 10,\ W = 10$ (c) $H = 50,\ W = 50$

Figure 1. Frozen-pair stability diagrams for three diagonal choices of (H, W). Stability/periodicity corresponds to $|A_s(V; H)| < 1$.

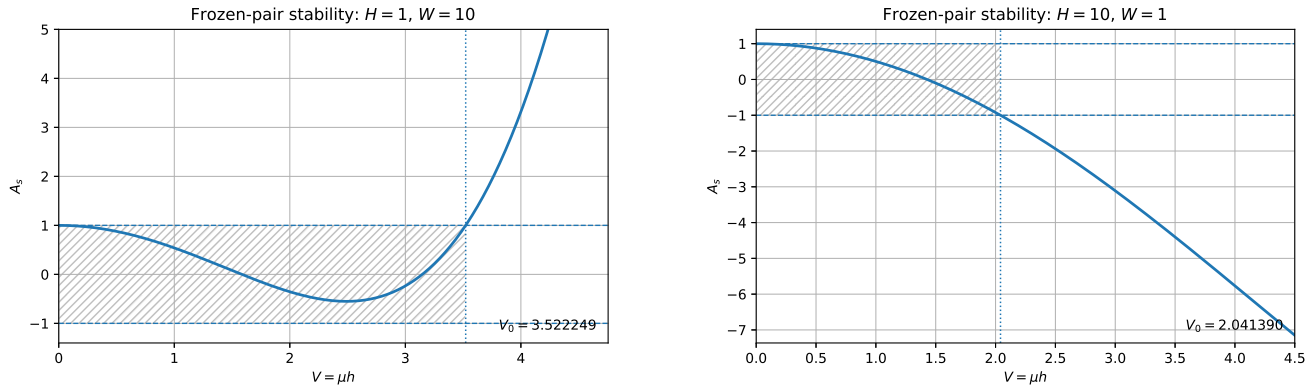

(a) $H = 1,\ W = 10$ (b) $H = 10,\ W = 1$

Figure 2. Off-diagonal fitted pairs. Comparison with Figure 1(a,b) demonstrates explicitly that changing W while holding H fixed does not alter the homogeneous stability set.

5.5. Dissipation

Because the constant term of the characteristic polynomial is one, $\zeta_1\zeta_2 = 1$. Inside every periodicity interval the two roots are complex conjugates, and therefore

$$|\zeta_1| = |\zeta_2| = 1. \tag{41}$$

Hence the method is nondissipative throughout every periodicity interval. Outside these intervals one of the reciprocal roots has modulus greater than one, so long integrations of the homogeneous probe problem are unstable.

Theorem 3 (Homogeneous stability and nondissipation)**.** *Freeze the fitted coefficients at (H, W) and apply the method to $y'' = -\mu^2 y$, $V = \mu h$. Then the characteristic equation is*

$$\boxed{\zeta^2 - 2A_s(V; H)\zeta + 1 = 0}$$

with

$$\boxed{\begin{aligned} A_s(V; H) &= 1 - \frac{V^2}{2} + \frac{c(H)}{2}V^4, \\ c(H) &= \frac{1 - S(H)}{H^2}. \end{aligned}}$$

Thus the frozen homogeneous stability function is independent of the forcing parameter W. The method is periodic and nondissipative whenever $|A_s(V; H)| < 1$. At the fitted point $V = H$ one has $A_s(H; H) = \cos H$.

The proof is given in Appendix C.

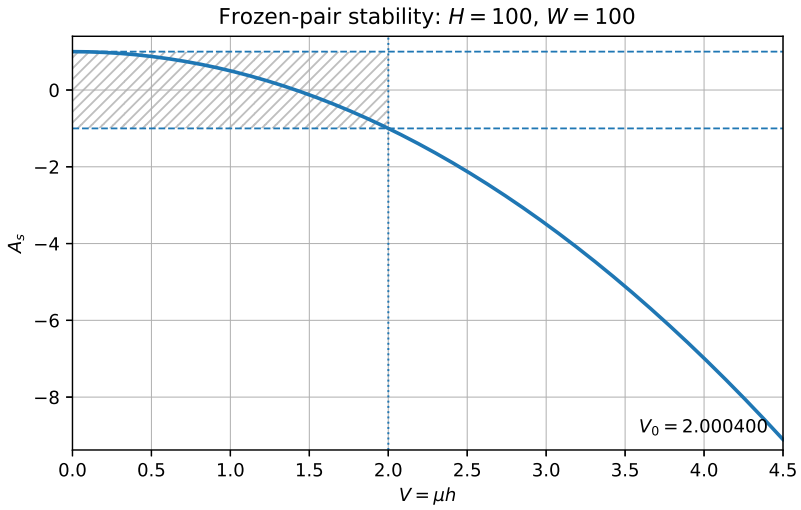

Figure 3. Frozen-pair stability diagram for $H = W = 100$. The first periodicity boundary is $V_0 = 2.0004002692$.

6. Local Truncation Error and Algebraic Order

For the local error calculation the exact values $y(x_{n-1})$ and $y(x_n)$ are inserted into one numerical step. For the general second-order problem

$$y'' = f(x, y), \tag{42}$$

we denote by

$$\boxed{f_y(x, y) = \frac{\partial f(x, y)}{\partial y}} \tag{43}$$

the partial derivative of the right-hand side with respect to the dependent variable y, while x is held fixed. Whenever f_y occurs in the local truncation error formulas below, it is evaluated along the exact solution at the mesh point x_n:

$$f_y \equiv f_y(x_n, y(x_n)) = \left.\frac{\partial f(x, y)}{\partial y}\right|_{x=x_n,\ y=y(x_n)}. \tag{44}$$

For the fitted model used in the construction of the new method,

$$f(x, y) = -\lambda^2 y + e^{i\omega x}, \tag{45}$$

and therefore

$$\boxed{f_y = -\lambda^2.} \tag{46}$$

If the right-hand side is independent of y, then $f_y = 0$.

We define the local defect as

$$\mathcal{T}_{n+1} = y(x_{n+1}) - 2y(x_n) + y(x_{n-1}) - h^2 \left[b_0 \left(f(x_{n+1}, y^p_{n+1}) + y''(x_{n-1})\right) + b_1 y''(x_n)\right]. \tag{47}$$

This convention is useful because the order of the unscaled defect is visible directly. If the local truncation error is defined after division by h^2, the expressions below must simply be divided by h^2.

For fixed physical frequencies λ and ω, with $H = \lambda h$ and $W = \omega h$, the fitted coefficients have the small-step expansions

$$b_0 = \frac{1}{12} + \frac{3\omega^2 - 2\lambda^2}{720} h^2 + O(h^4), \tag{48}$$

$$b_1 = \frac{5}{6} - \frac{3\omega^2 - 2\lambda^2}{360} h^2 + O(h^4), \tag{49}$$

$$a = 1 - \frac{\omega^2}{20} h^2 + O(h^4). \tag{50}$$

The predictor generated from exact starting values consequently satisfies

$$y^p_{n+1} - y(x_{n+1}) = -h^4 \left[\frac{y^{(4)}(x_n)}{12} + \frac{\omega^2 y''(x_n)}{20}\right] + O(h^5). \tag{51}$$

Taylor expansion of the corrector then gives the leading local defect of the new method:

$$\boxed{\mathcal{T}_{n+1}^{\text{new}} = h^6\left[-\frac{1}{240}y^{(6)} + \left(\frac{f_y}{144} + \frac{\lambda^2}{360} - \frac{\omega^2}{240}\right)y^{(4)} + \frac{f_y\omega^2}{240}y''\right]_{x=x_n} + O(h^7).} \tag{52}$$

Thus the unscaled local defect is $O(h^6)$ and the method has fourth algebraic order in the usual two-step second-order convention.

For the classical member, obtained by taking $H = W = 0$, one has

$$a = 1, \qquad b_0 = \frac{1}{12}, \qquad b_1 = \frac{5}{6}. \tag{53}$$

Its corresponding local defect is

$$\boxed{\mathcal{T}_{n+1}^{\text{class}} = h^6\left[-\frac{1}{240}y^{(6)} + \frac{f_y}{144}y^{(4)}\right]_{x=x_n} + O(h^7).} \tag{54}$$

For equations whose right-hand side is independent of y, $f_y = 0$, this reduces to the familiar Numerov leading term

$$\mathcal{T}_{n+1}^{\text{class}} = -\frac{h^6}{240}y^{(6)}(x_n) + O(h^7). \tag{55}$$

The extra f_y term in (54) is due to the explicit predictor used to evaluate the endpoint acceleration; it is absent in the implicit Numerov formula when the exact endpoint acceleration is used.

The fitted expression (52) has an important consistency check. For the construction equation

$$y'' = -\lambda^2 y + e^{i\omega x}, \qquad f_y = -\lambda^2, \tag{56}$$

the differential identities implied by this equation make the coefficient of h^6 in (52) vanish. In fact, the result is stronger: because the numerical and exact grid recurrences coincide, the local grid defect is identically zero on the complete fitted test space in exact arithmetic.

A particularly transparent comparison is obtained from the homogeneous probe $y'' = -\mu^2 y$. In this case,

$$\mathcal{T}_{n+1}^{\text{new}} = \frac{\mu^4(\lambda^2 - \mu^2)}{360}h^6 y(x_n) + O(h^7), \tag{57}$$

whereas the classical explicit predictor–corrector gives

$$\mathcal{T}_{n+1}^{\text{class}} = -\frac{\mu^6}{360}h^6 y(x_n) + O(h^7). \tag{58}$$

Equation (57) displays directly the phase-fitting property: the leading defect vanishes at the selected natural frequency $\mu = \lambda$.

Theorem 4 (Local truncation error and algebraic order)**.** *For $y'' = f(x, y)$, with $f_y = \partial f/\partial y$ evaluated along the exact solution, the unscaled local defect of the new method satisfies*

$$\mathcal{T}_{n+1}^{\text{new}} = h^6\left[-\frac{1}{240}y^{(6)} + \left(\frac{f_y}{144} + \frac{\lambda^2}{360} - \frac{\omega^2}{240}\right)y^{(4)} + \frac{f_y\omega^2}{240}y''\right]_{x=x_n} + O(h^7).$$

Hence the method has local algebraic order four in the usual two-step second-order convention; global fourth-order convergence requires the regularity and starting-value assumptions stated in the conditional convergence theorem in Appendix 11. For the fitted equation $f_y = -\lambda^2$ the leading coefficient vanishes, and in fact the complete grid defect vanishes identically on the fitted test space.

Corollary 1 (Homogeneous fitted probe)**.** *For $y'' = -\mu^2 y$,*

$$\mathcal{T}_{n+1}^{\text{new}} = \frac{\mu^4(\lambda^2 - \mu^2)}{360}h^6 y(x_n) + O(h^7),$$

so the leading defect vanishes for $\mu = \lambda$.

The proof of Theorem 4 and Corollary 1 is given in Appendix D.

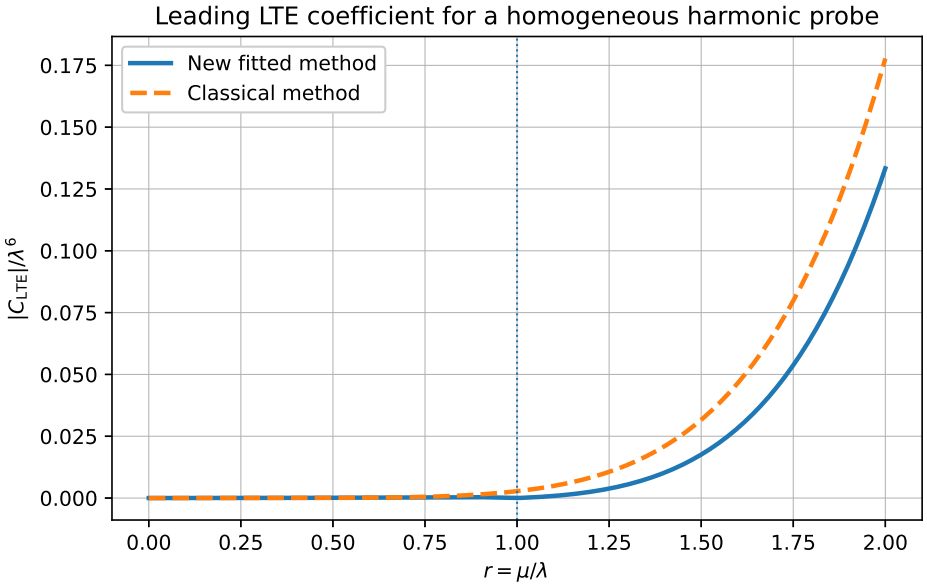

Figure 4. Magnitude of the normalized leading LTE coefficient for the homogeneous probe $y'' = -\mu^2 y$, with $r = \mu/\lambda$. The fitted method has coefficient $|r^4(1-r^2)|/360$, whereas the classical explicit Numerov-type predictor–corrector has coefficient $r^6/360$.

7. Implementation and Experimental Protocol

For constant stepsize and fixed fitted frequencies, the quantities H, W, a, b_0 and b_1 are calculated once before the integration starts. The sinc form of Φ is used for ordinary arguments, the diagonal limit is used when H and W are close, and the corresponding series are used near the origin.

Since the formula is two-step, one additional starting value is required. In all experiments this value is computed with sufficient accuracy so that the starting procedure does not affect the reported results. For nonlinear problems without a closed exact solution, the final error is measured against an independently computed high-accuracy reference solution.

The work–precision diagrams use CPU time on the abscissa and $-\log_{10}(\text{error})$ on the ordinate. Nonfinite errors and failed integrations are omitted. The same computational-method notation is used in all numerical examples:

Method	Formula
Computational Method I	Classical Numerov IPL3 [2]
Computational Method II	RKDP4 [10]
Computational Method III	RKDP5 [10]
Computational Method IV	RKDP6 [13]
Computational Method V	RKFE4 [14]
Computational Method VI	RKFE5 [14, 15]
Computational Method VII	RKFE6 [15]
Computational Method VIII	Chawla–Rao [9]
Computational Method IX	New Numerov IPL3 method

The Dormand–Prince comparisons use the published Dormand–Prince family and its higher-order extension [10, 13]; the Fehlberg comparisons use the corresponding classical embedded Runge–Kutta families [14, 15]; and Computational Method VIII is the explicit minimal-phase-lag Numerov-type formula of Chawla and Rao [9]. The labels RKDP4, RKDP5, RKDP6 and RKFE4, RKFE5, RKFE6 in the present paper refer to the particular output formulae implemented in the experiments, rather than to a claim that each label is the title used in the original publications.

8. Numerical Experiments

We now study the numerical behavior of the new formula on eight problems. The first two are scalar equations and the remaining six are systems with eight or ten second-order equations. The set contains problems which belong exactly to the fitting class and problems with nonlinear terms or weak couplings which are not included in the test equation.

For the linear problems the exact solution is used in the error calculation. For the nonlinear problems a separately computed reference solution is used. The fitted frequencies are chosen from the dominant natural and forcing frequencies stated in each example. The results are presented as work–precision diagrams using the notation of Section 7.

The provenance of the test set is stated explicitly. The exact scalar forced-oscillator benchmark is a frequency-scaled version of a standard inhomogeneous oscillatory test problem used in the fitted-integrator literature [1, 2]. The weakly nonlinear Duffing oscillator is a perturbation introduced here from the same forced-oscillator structure, rather than a problem quoted verbatim from an earlier paper. The six system benchmarks were constructed for the present study from standard modal models: independent forced oscillators, a semidiscrete wave equation, a spring–mass chain, a weakly nonlinear lattice, generalized structural dynamics, and a weakly coupled oscillatory system. References cited in the corresponding subsections document these mathematical model classes, not the particular numerical constants chosen here.

8.1. Exact two-frequency periodically forced oscillator

We first consider a frequency-scaled form of the standard inhomogeneous oscillatory benchmark used in earlier studies of periodically forced and fitted integrators [1, 2]:

$$y'' = -10000y + 9999\sin x, \qquad y(0) = 1, \qquad y'(0) = 101, \tag{59}$$

on the long interval $0 \le x \le 100000$. In the notation of the fitted model, $\lambda = 100$ and $\omega = 1$, and therefore

$$H = 100h, \qquad W = h. \tag{60}$$

The complementary solution is

$$y_h(x) = A_1\cos(100x) + A_2\sin(100x), \tag{61}$$

while a particular solution is $y_p(x) = \sin x$. The initial conditions give $A_1 = A_2 = 1$ and hence the analytical solution is

$$y(x) = \cos(100x) + \sin(100x) + \sin x. \tag{62}$$

Thus the error can be evaluated directly, without a numerical reference solution. This example contains the natural and forcing frequencies independently and belongs exactly to the two-frequency model used in the construction of Computational Method IX. It is consequently the most direct test of the inhomogeneous response-fitting mechanism. Figure 5 presents the corresponding work–precision diagram.

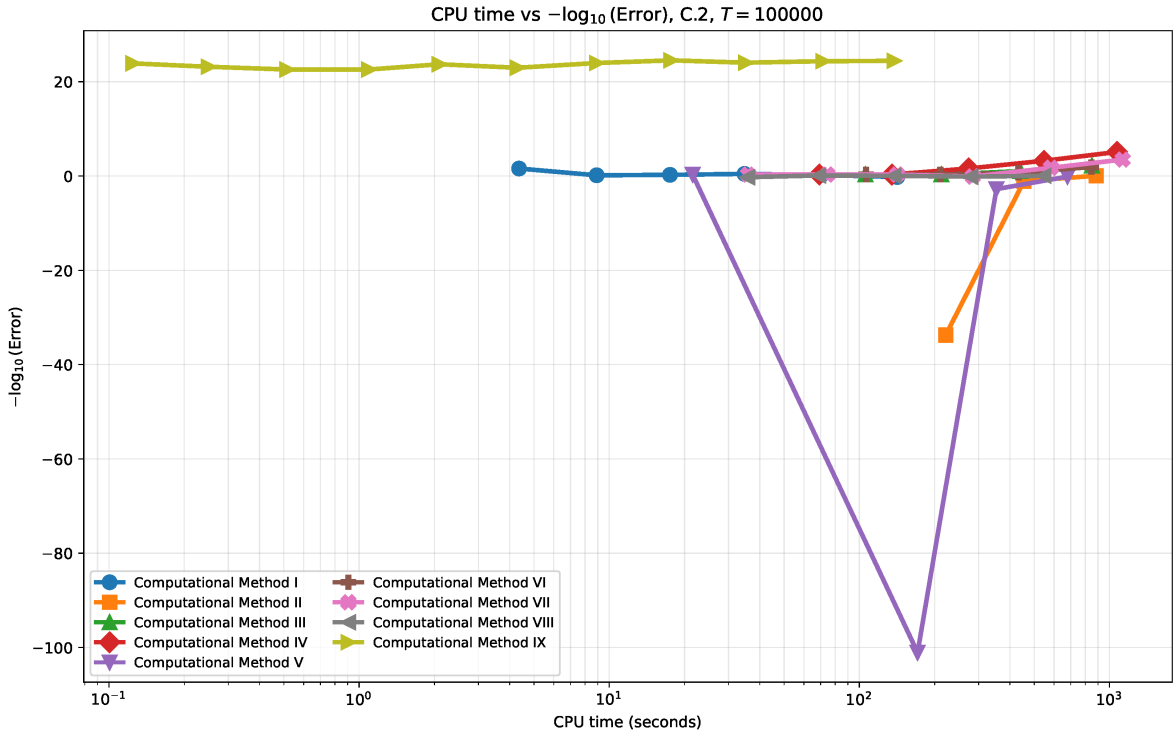

Figure 5. Exact two-frequency periodically forced oscillator: CPU time versus $-\log_{10}(E)$ for Computational Methods I–IX, $T = 100000$.

8.2. Weakly nonlinear forced Duffing oscillator

The second scalar model is a weakly nonlinear Duffing-type perturbation constructed for the present experiments from the preceding forced-oscillator benchmark. Duffing equations are standard nonlinear oscillatory tests in the fitted-integrator literature; representative uses and background may be found in [5, 17, 19]. Thus, the particular coefficients and initial data below are part of the present test set rather than a verbatim problem taken from an earlier source:

$$y'' + 100y + 10^{-2}y^3 = 99\sin x, \qquad y(0) = 1, \qquad y'(0) = 11, \tag{63}$$

for $0 \le x \le 10000$. If the cubic term is suppressed, the associated linear problem is

$$y'' + 100y = 99 \sin x, \tag{64}$$

with analytical solution

$$y_{\text{lin}}(x) = \cos(10x) + \sin(10x) + \sin x. \tag{65}$$

The linear part therefore identifies the natural and forcing frequencies as

$$\lambda = 10, \qquad \omega = 1, \qquad H = 10h, \qquad W = h. \tag{66}$$

For the nonlinear equation no elementary closed-form solution is available. The numerical experiments therefore use an independently generated high-accuracy reference; at the final point the reference value employed is

$$y(10000) \simeq -0.25706140835. \tag{67}$$

The linear analytical solution above explains the fitted frequencies, whereas the reference solution measures the effect of the weak cubic perturbation. Figure 6 shows the corresponding efficiency results.

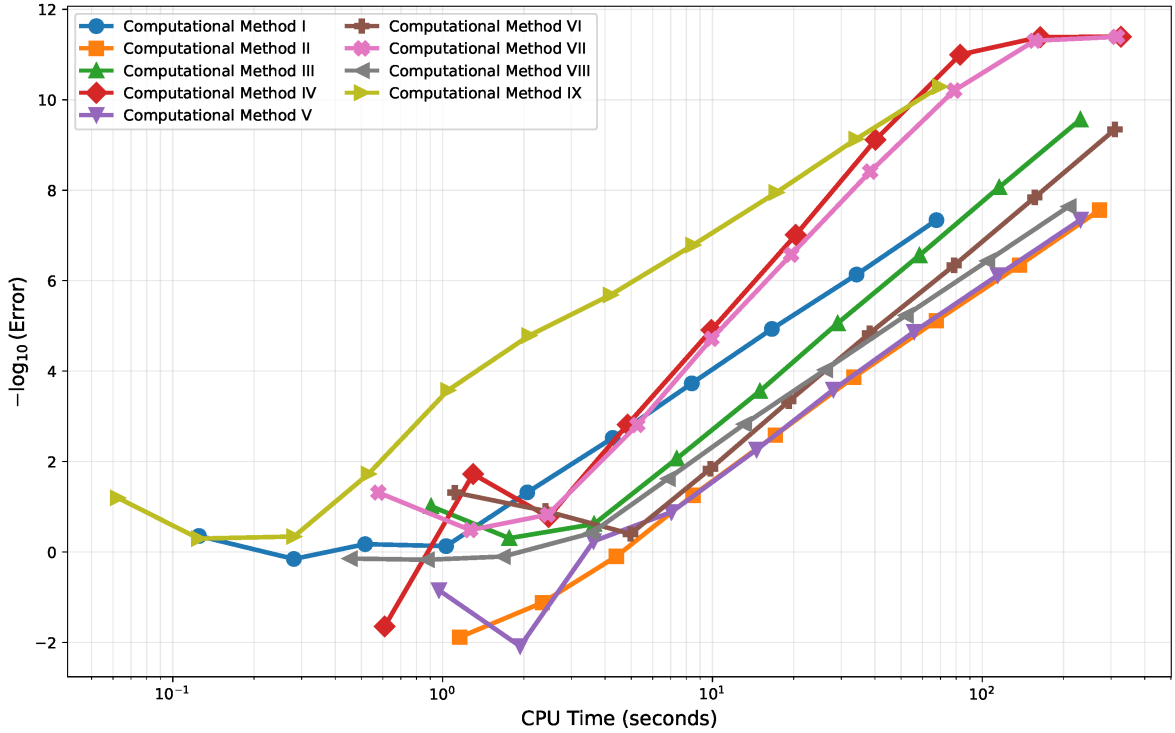

Figure 6. Weakly nonlinear forced Duffing oscillator: CPU time versus $-\log_{10}(E)$ for Computational Methods I–IX, $T = 10000$.

8.3. Ten independent periodically forced oscillators

This ten-component benchmark is constructed here by taking ten independent copies of the two-frequency forced oscillator with different forcing amplitudes. Its model class is the vector counterpart of periodically forced second-order systems considered in fitted integration; see, for example, [1, 17]. The numerical constants used below are specific to the present benchmark.

Let $\mathbf{y} = (y_1, \ldots, y_{10})^T \in \mathbb{R}^{10}$ satisfy

$$\mathbf{y}'' + \lambda^2 \mathbf{y} = \mathbf{c} \cos(\omega x) + \mathbf{d} \sin(\omega x), \qquad 0 \le x \le 200, \tag{68}$$

where

$$\lambda = 50, \qquad \omega = 3, \tag{69}$$

$$\mathbf{c} = (1, 2, 3, 4, 5, 6, 7, 8, 9, 10)^T, \qquad \mathbf{d} = (10, 9, 8, 7, 6, 5, 4, 3, 2, 1)^T, \tag{70}$$

and

$$\mathbf{A} = (1, 1, 1, 1, 1, 1, 1, 1, 1, 1)^T, \qquad \mathbf{B} = 0.05(1, 2, 3, 4, 5, 6, 7, 8, 9, 10)^T. \tag{71}$$

Since $\lambda^2 - \omega^2 = 2500 - 9 = 2491$, the exact vector solution is

$$\mathbf{y}(x) = \mathbf{A} \cos(50x) + \mathbf{B} \sin(50x) + \frac{\mathbf{c} \cos(3x) + \mathbf{d} \sin(3x)}{2491}. \tag{72}$$

Consequently,

$$\mathbf{y}(0) = \mathbf{A} + \frac{\mathbf{c}}{2491}, \qquad \mathbf{y}'(0) = 50\mathbf{B} + \frac{3\mathbf{d}}{2491}. \tag{73}$$

The fitting parameters are $H = 50h$ and $W = 3h$. Since all ten components have the same two-frequency form, this problem is an exact vector realization of the scalar fitting model and no numerical reference solution is required. The endpoint error is evaluated from the analytical expression above. Figure 7 gives the work–precision results.

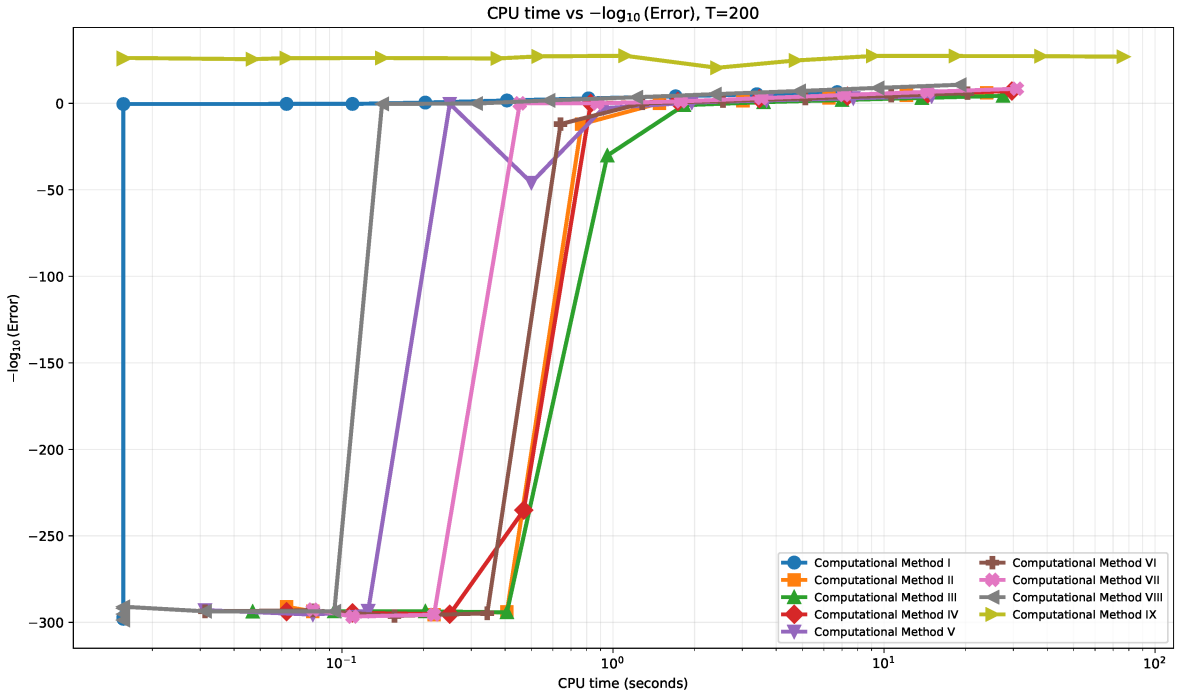

Figure 7. Ten independent periodically forced oscillators: CPU time versus $-\log_{10}(E)$ for Computational Methods I–IX, $T = 200$.

8.4. Ten-node semidiscrete forced wave equation

This benchmark is constructed here by applying the standard centered spatial semidiscretization to a forced wave equation and exciting one discrete eigenmode. Such spatial discretizations lead to highly oscillatory second-order ODE systems, for which specialized RKN/exponential integrators are widely used; see [17, 18]. The ten-node instance and its constants are chosen here.

Consider the forced wave equation

$$u_{tt} = c^2 u_{xx} + F(x)\cos(\omega t), \qquad 0 < x < 1, \tag{74}$$

with homogeneous Dirichlet boundary conditions. Using ten interior nodes, $\Delta x = 1/11$, and the standard centered spatial discretization gives

$$\mathbf{u}'' = -K\mathbf{u} + F_0\boldsymbol{\phi}_4\cos(\omega t), \qquad K = \frac{c^2}{\Delta x^2}\,\mathrm{tridiag}(-1, 2, -1). \tag{75}$$

For $c = 10$, $F_0 = 2$, $\omega = 3$ and mode $k = 4$, let the Euclidean-normalized eigenvector be

$$(\boldsymbol{\phi}_4)_j \propto \sin\left(\frac{4j\pi}{11}\right), \qquad j = 1, \ldots, 10. \tag{76}$$

Its discrete modal frequency is

$$\lambda_4 = \frac{2c}{\Delta x}\sin\left(\frac{4\pi}{22}\right) \simeq 118.9409798402. \tag{77}$$

Because the initial data and forcing are parallel to $\boldsymbol{\phi}_4$, the solution remains exactly in this eigenspace. Writing $\mathbf{u}(t) = q(t)\boldsymbol{\phi}_4$, the ten-dimensional system reduces to

$$q'' + \lambda_4^2 q = 2\cos(3t). \tag{78}$$

With the prescribed modal data the exact amplitude is

$$q(t) = \cos(\lambda_4 t) + 0.3\sin(\lambda_4 t) + \frac{2\cos(3t)}{\lambda_4^2 - 9}. \tag{79}$$

Thus

$$\mathbf{u}(0) = \left(1 + \frac{2}{\lambda_4^2 - 9}\right)\boldsymbol{\phi}_4, \qquad \mathbf{u}'(0) = 0.3\lambda_4\boldsymbol{\phi}_4, \tag{80}$$

and the fitted parameters are $H = \lambda_4 h$ and $W = 3h$. The analytical modal solution is used directly in the endpoint error. Figure 8 reports the measured efficiency.

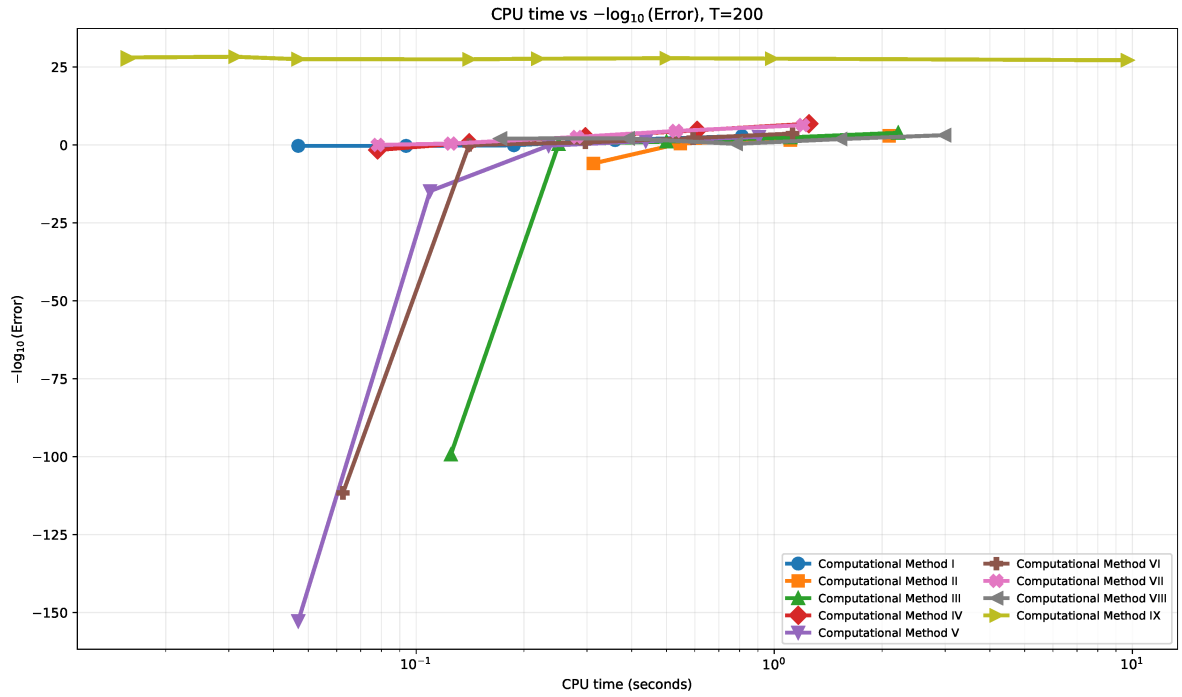

Figure 8. Ten-node semidiscrete forced wave equation: CPU time versus $-\log_{10}(E)$ for Computational Methods I–IX, $T = 200$.

8.5. Ten-mass periodically forced spring chain

This benchmark is constructed here from the standard nearest-neighbor spring–mass matrix and a single forced normal mode. Spring–mass and vibration models belong to the standard class of oscillatory second-order systems motivating fitted and phase-adapted integrators [3, 17, 18]. The particular ten-mass data below are introduced for the present comparison.

For ten equal masses we consider

$$\mathbf{y}'' + K\mathbf{y} = F_0\boldsymbol{\phi}_7\cos(\omega x), \qquad K = \kappa\,\mathrm{tridiag}(-1, 2, -1), \tag{81}$$

with $\kappa = 10000$, $F_0 = 1.5$ and $\omega = 2$. The normal frequencies are

$$\lambda_k = 2\sqrt{\kappa}\sin\left(\frac{k\pi}{22}\right), \tag{82}$$

and for the selected seventh mode

$$\lambda_7 \simeq 168.2507065662. \tag{83}$$

Taking the initial data and the forcing in the direction of the Euclidean-normalized eigenvector $\boldsymbol{\phi}_7$ gives $\mathbf{y}(x) = q(x)\boldsymbol{\phi}_7$, where

$$q'' + \lambda_7^2 q = 1.5\cos(2x). \tag{84}$$

The exact modal amplitude used in the experiment is

$$q(x) = 0.8\cos(\lambda_7 x) + 0.2\sin(\lambda_7 x) + \frac{1.5\cos(2x)}{\lambda_7^2 - 4}. \tag{85}$$

Hence

$$\mathbf{y}(0) = \left(0.8 + \frac{1.5}{\lambda_7^2 - 4}\right)\boldsymbol{\phi}_7, \qquad \mathbf{y}'(0) = 0.2\lambda_7\boldsymbol{\phi}_7. \tag{86}$$

The fitting values are $H = \lambda_7 h$ and $W = 2h$. The reduction to the scalar fitted oscillator is exact, so the analytical modal solution supplies the reference endpoint. Figure 9 shows the results.

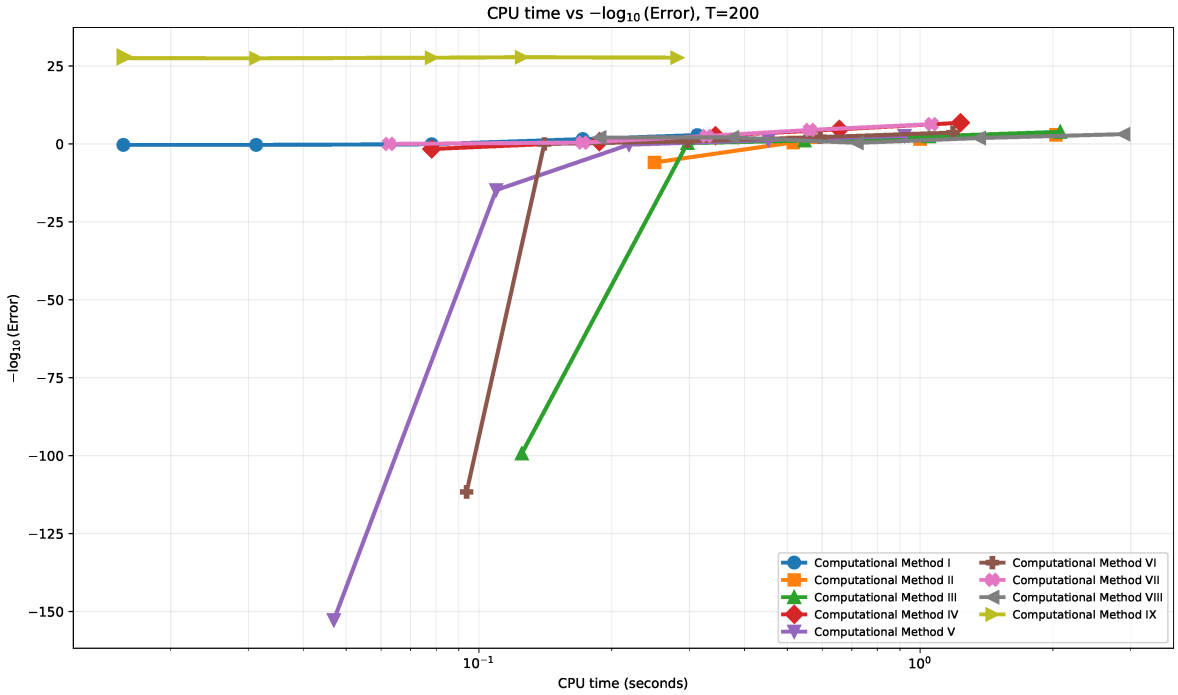

Figure 9. Ten-mass periodically forced spring chain: CPU time versus $-\log_{10}(E)$ for Computational Methods I–IX, $T = 200$.

8.6. Weakly nonlinear ten-mass lattice

This benchmark is constructed here by adding a weak componentwise cubic perturbation to the preceding modal lattice. Weakly nonlinear oscillators and Duffing-type cubic perturbations are established tests for oscillatory integrators [5, 17, 19]; here the same idea is extended to a ten-component lattice with the numerical parameters specified below.

The nonlinear lattice is

$$\mathbf{y}'' + K\mathbf{y} + \varepsilon \mathbf{y}^{\circ 3} = F_0 \boldsymbol{\phi}_4 \cos(2x), \tag{87}$$

where

$$K = 100\,\mathrm{tridiag}(-1, 2, -1), \qquad \varepsilon = 10^{-4}, \qquad F_0 = 1. \tag{88}$$

Here $\mathbf{y}^{\circ 3} = (y_1^3, \ldots, y_{10}^3)^T$. The fourth linear mode is used, with

$$\lambda_4 = 20 \sin\left(\frac{2\pi}{11}\right) \simeq 10.8128, \qquad H = \lambda_4 h, \qquad W = 2h, \tag{89}$$

and the initial data are

$$\mathbf{y}(0) = \boldsymbol{\phi}_4, \qquad \mathbf{y}'(0) = 0.2\lambda_4 \boldsymbol{\phi}_4. \tag{90}$$

If $\varepsilon = 0$, the motion remains in the fourth eigenspace and the corresponding linear analytical approximation is

$$\mathbf{y}_{\mathrm{lin}}(x) = q_{\mathrm{lin}}(x)\boldsymbol{\phi}_4, \tag{91}$$

where

$$q_{\mathrm{lin}}(x) = \cos(\lambda_4 x) + 0.2\sin(\lambda_4 x) + \frac{\cos(2x) - \cos(\lambda_4 x)}{\lambda_4^2 - 4}. \tag{92}$$

For $\varepsilon = 10^{-4}$ the componentwise cubic term destroys exact modal invariance; therefore this expression is only the natural linear approximation, not the exact solution of the experiment. The numerical errors are computed against an independently generated tight-tolerance reference solution on $0 \le x \le 200$. Figure 10 gives the work–precision diagram.

8.7. Eight-degree-of-freedom structural dynamics problem

This benchmark is constructed here as a generalized modal structural-dynamics problem with a nonidentity mass matrix. Direct integration of second-order systems $M\mathbf{y}'' + K\mathbf{y} = \mathbf{f}(x)$ and the importance of stability and phase properties in structural dynamics are discussed, for example, in [18]. The mass matrix, stiffness matrix and selected modal data used here are specific to the present experiment.

We next consider the generalized structural system

$$M\mathbf{y}'' + K\mathbf{y} = F_0 M \boldsymbol{\phi}_4 \cos(\omega x), \tag{93}$$

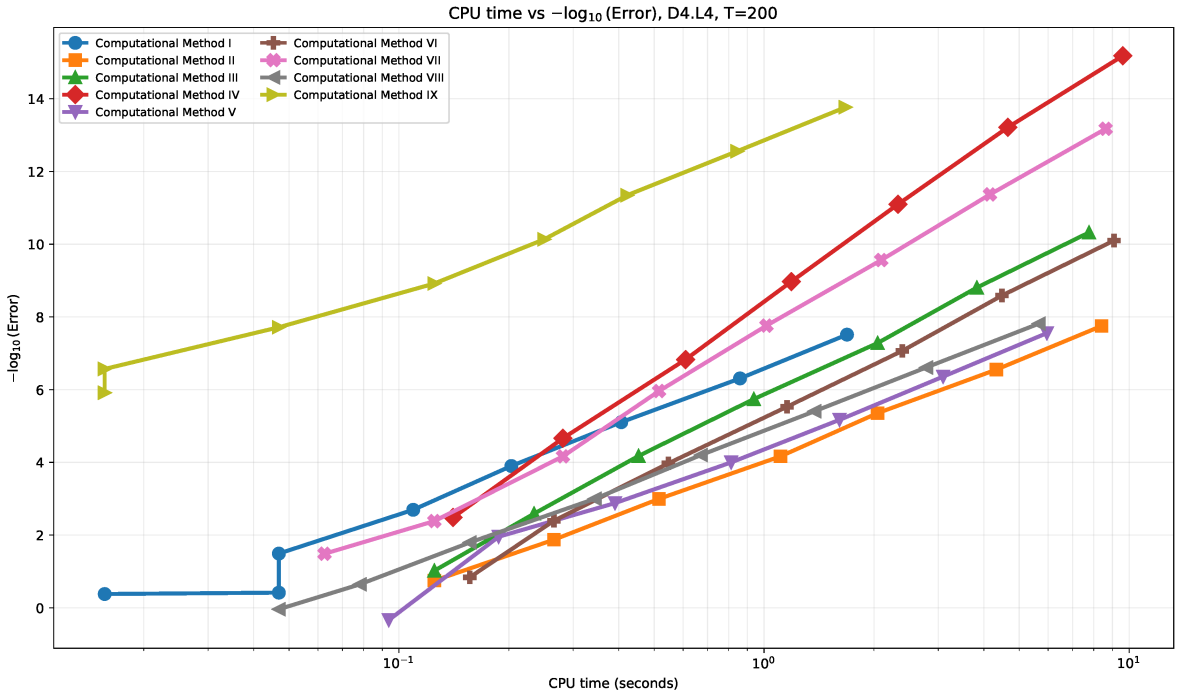

Figure 10. Weakly nonlinear ten-mass lattice: CPU time versus $-\log_{10}(E)$ for Computational Methods I–IX, $T = 200$.

with

$$M = \mathrm{diag}(1, 2, 1.5, 2.5, 1, 3, 2, 1.5), \qquad K = 400\,\mathrm{tridiag}(-1, 2, -1), \tag{94}$$

$F_0 = 1.2$ and $\omega = 2.5$. The generalized modes satisfy

$$K\boldsymbol{\phi}_k = \lambda_k^2 M\boldsymbol{\phi}_k, \tag{95}$$

with $\boldsymbol{\phi}_4^T M\boldsymbol{\phi}_4 = 1$. For the fourth mode,

$$\lambda_4 \simeq 18.4982430304, \qquad H = \lambda_4 h, \qquad W = 2.5h. \tag{96}$$

Since both the initial data and forcing are modal, $\mathbf{y}(x) = q(x)\boldsymbol{\phi}_4$ exactly, and the scalar amplitude satisfies

$$q'' + \lambda_4^2 q = 1.2\cos(2.5x). \tag{97}$$

The analytical amplitude is

$$q(x) = 0.7\cos(\lambda_4 x) + 0.15\sin(\lambda_4 x) + \frac{1.2\cos(2.5x)}{\lambda_4^2 - 2.5^2}. \tag{98}$$

Therefore

$$\mathbf{y}(0) = \left(0.7 + \frac{1.2}{\lambda_4^2 - 2.5^2}\right)\boldsymbol{\phi}_4, \qquad \mathbf{y}'(0) = 0.15\lambda_4\boldsymbol{\phi}_4. \tag{99}$$

This example preserves exact modal fitting while introducing a nonidentity mass matrix. Figure 11 presents the efficiency diagram.

8.8. Weakly coupled ten-equation oscillatory system

This final benchmark is constructed here as a weakly coupled perturbation of ten identical forced oscillators. Weakly coupled/highly oscillatory second-order systems are a natural extension of the fitted-oscillator setting and are covered by the broader exponential-fitting and oscillatory-integration literature [3, 17]. The decaying nearest-neighbor coupling and the numerical constants below are introduced for the present test.

Finally, let $\mathbf{y} \in \mathbb{C}^{10}$ satisfy

$$\mathbf{y}'' = -20^2\mathbf{y} + 10^{-3}e^{-0.01x}C\mathbf{y} + \mathbf{f}e^{3ix}, \qquad 0 \le x \le 200, \tag{100}$$

where C is the symmetric nearest-neighbor matrix with ones on the first super- and sub-diagonals and

$$\mathbf{f} = \frac{(1, 2, \ldots, 10)^T}{\sqrt{385}}. \tag{101}$$

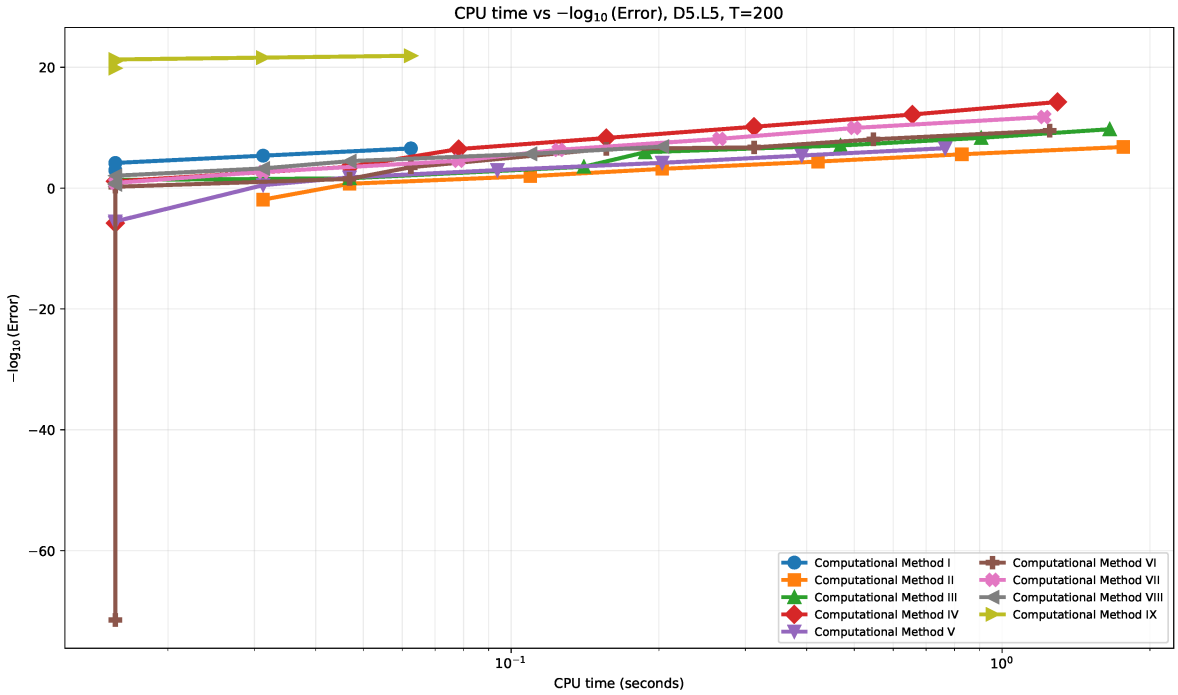

Figure 11. Eight-degree-of-freedom structural dynamics problem: CPU time versus $-\log_{10}(E)$ for Computational Methods I–IX, $T = 200$.

The initial data are

$$\mathbf{y}(0) = \frac{1}{\sqrt{10}}(1, \ldots, 1)^T, \qquad \mathbf{y}'(0) = \frac{0.2i}{\sqrt{10}}(1, \ldots, 1)^T. \tag{102}$$

The dominant uncoupled oscillator has

$$\lambda = 20, \qquad \omega = 3, \qquad H = 20h, \qquad W = 3h. \tag{103}$$

If the coupling term is omitted, an analytical reference for the principal model is obtained from

$$\mathbf{y}_0'' + 400\mathbf{y}_0 = \mathbf{f}e^{3ix}. \tag{104}$$

Writing $\mathbf{y}_0 = \mathbf{A}\cos(20x) + \mathbf{B}\sin(20x) + \mathbf{f}e^{3ix}/391$, the initial conditions give

$$\mathbf{A} = \mathbf{y}(0) - \frac{\mathbf{f}}{391}, \qquad \mathbf{B} = \frac{\mathbf{y}'(0) - 3i\mathbf{f}/391}{20}. \tag{105}$$

Thus $\mathbf{y}_0(x)$ is the analytical uncoupled approximation. The decaying term $10^{-3}e^{-0.01x}C\mathbf{y}$ makes the actual problem a weakly coupled perturbation, so no closed-form solution is used for the reported errors. Instead, an independent tight-tolerance numerical reference is employed. Figure 12 gives the corresponding work–precision diagram.

8.9. Interpretation of the complete numerical set

The eight experiments distinguish exact fitting from nonlinear and weakly coupled behavior. The exact scalar forced oscillator is most closely aligned with the derivation; the weakly nonlinear Duffing oscillator and lattice deliberately perturb the fitted linear structure. The independent forced oscillators, semidiscrete wave equation, and spring–mass chain examine the extension of scalar fitting to systems. The structural dynamics example tests a generalized eigenproblem, while the weakly coupled oscillatory system introduces coupling. All eight work–precision diagrams use the same Computational Methods I–IX labeling, permitting direct comparison across the test set.

9. Discussion

The coefficient relations show that the two fitted frequencies have different roles. The parameter H determines the homogeneous propagation, whereas W is required to reproduce the inhomogeneous response. After use of the normalization, the product ab_0 depends only on H. This explains why the frozen homogeneous stability function is independent of W even though the individual coefficients are not.

The numerical experiments also separate these two effects. When the frequencies used in the construction are the actual dominant frequencies of the problem, the fitted grid components are treated with very small error. For

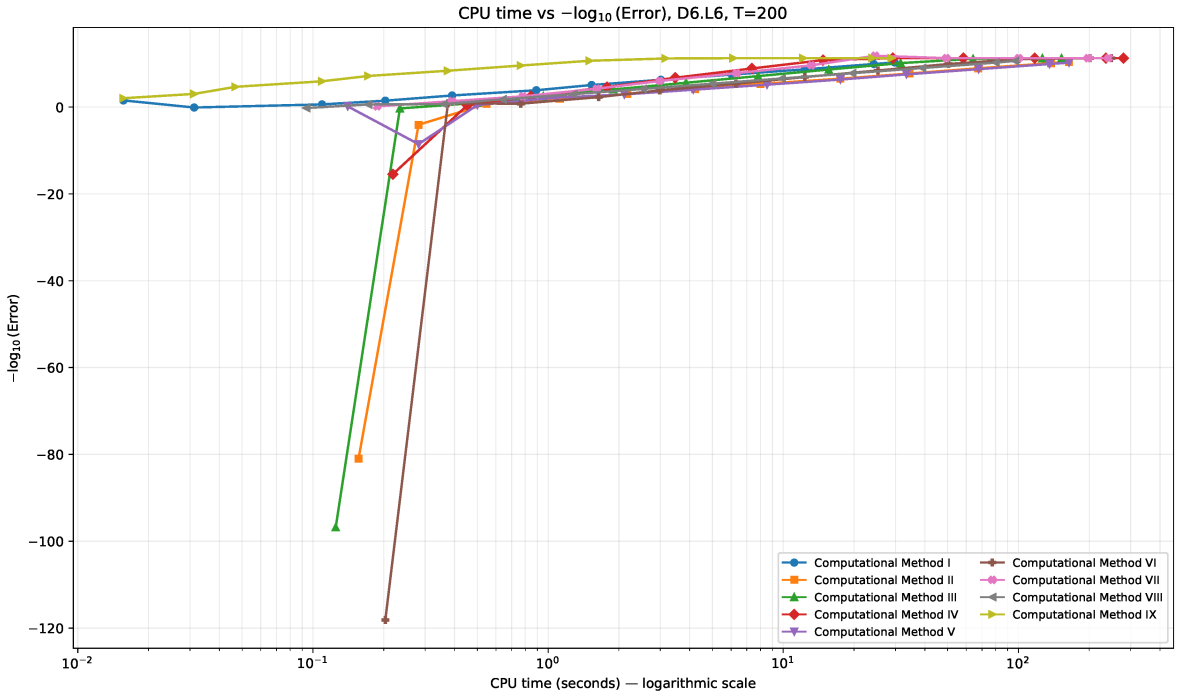

Figure 12. Weakly coupled ten-equation oscillatory system: CPU time versus $-\log_{10}(E)$ for Computational Methods I–IX, $T = 200$.

the nonlinear and weakly coupled problems the fitting is only approximate, and the advantage depends on how well the selected frequencies describe the solution.

Finally, the limiting formulae used for the coefficients are important in long integrations. Direct evaluation of removable quotients near $H = W$ or near the origin can destroy the accuracy which is obtained analytically.

10. Conclusions

In this paper we have developed an explicit Numerov-type method for second-order oscillatory initial value problems with periodic forcing. The construction uses the two independent quantities $H = \lambda h$ and $W = \omega h$. Application of the predictor–corrector to $y'' = -\lambda^2 y + \exp(i\omega x)$ and comparison with the exact grid difference equation give closed formulae for a, b_0 and b_1.

The limit $W = H$ was obtained by continuity and the classical Numerov coefficients were recovered as $H, W \to 0$. The stability analysis showed that the homogeneous periodicity function depends only on H and that the method is nondissipative inside its periodicity intervals. The local truncation error gives fourth algebraic order, while the fitted test space is reproduced exactly at the grid points.

The numerical study comprised two scalar oscillators (an exact periodically forced problem and a weakly nonlinear Duffing perturbation) and six systems (independent forced oscillators, a semidiscrete wave equation, a spring–mass chain, a nonlinear lattice, structural dynamics, and a weakly coupled oscillatory system). Comparisons with the eight baseline Computational Methods I–VIII, alongside the proposed Computational Method IX, illustrate the benefits of fitting the dominant oscillatory frequencies and the behavior when nonlinear or coupled terms depart from the fitted model.

11. Conditional global convergence

Conditional global fourth-order convergence (fixed fitting frequencies)

Theorem 5 (Global convergence under standard starting assumptions)**.** *Let $y'' = f(x, y)$ on a finite interval $[x_0, T]$, with f uniformly Lipschitz in y on a neighborhood of the exact solution, and assume sufficient smoothness for a uniform local defect $|\mathcal{T}_{n+1}| \le Ch^6$. Fix finite λ, ω independent of h, and evaluate the coefficient functions by their analytic continuations for sufficiently small h, so that a, b_0, b_1 remain uniformly bounded. If $|y_0 - y(x_0)| \le C_0 h^4$ and $|(y_1 - y(x_1)) - (y_0 - y(x_0))| \le C_0 h^5$, then for sufficiently small h,*

$$\max_{0 \le n \le (T-x_0)/h} |y_n - y(x_n)| \le C_T h^4.$$

Proof. Write $e_n = y_n - y(x_n)$. The predictor perturbation is bounded by $|\delta p_{n+1}| \le 2|e_n| + |e_{n-1}| + Ch^2|e_n|$ using Lipschitz continuity and bounded a. Consequently, subtracting the exact-solution defect equation from the corrector gives

$$|e_{n+1} - 2e_n + e_{n-1}| \le Ch^2(|e_n| + |e_{n-1}|) + Ch^6.$$

The discrete Green function for the second-difference operator with zero initial data is $G_{n,j} = n - j$, and hence

$$|e_n| \le |e_0| + n|e_1 - e_0| + Ch^2 \sum_{j=1}^{n-1} (n-j)(|e_j| + |e_{j-1}|) + Ch^6 \sum_{j=1}^{n-1} (n-j).$$

For fourth-order global accuracy one needs the sharper starting condition $|e_0| \le C_0 h^4$ and $|e_1 - e_0| \le C_0 h^5$, not merely $|e_0| + |e_1| = O(h^4)$. Under this strengthened hypothesis the free term is $O(h^4)$ for $nh \le T - x_0$. The discrete Volterra inequality, equivalently a discrete Gronwall bound for the associated first-order scaled-error system, yields $\max_n |e_n| \le C_T h^4$. □

Funding

The authors gratefully acknowledge the Deanship of Scientific Research (DSR) at King Abdulaziz University, Jeddah, Saudi Arabia, for funding this project under grant No. (IPP: 1685-135-2025) and for providing technical support.

Apendices

A. Proof of Theorem 1

The proof is organized through two intermediate results. The first gives the numerical recurrence produced by the predictor–corrector, while the second gives the exact grid recurrence of the fitting equation.

Lemma 1 (Numerical recurrence)**.** *For the fitting equation and arbitrary coefficients satisfying* $2b_0 + b_1 = 1$*, application of the predictor–corrector gives*

$$\boxed{y_{n+1} - \left[2 - H^2(1 - ab_0H^2)\right] y_n + y_{n-1} = h^2 \left[1 - ab_0H^2 - 4b_0 \sin^2(W/2)\right] e^{i\omega x_n}.}$$

Lemma 2 (Exact grid recurrence)**.** *For* $H \neq W$*, every exact solution of* $y'' = -\lambda^2 y + e^{i\omega x}$ *satisfies*

$$y_{n+1} - 2\cos(H)y_n + y_{n-1} = h^2\Phi(H, W)e^{i\omega x_n}, \qquad \Phi(H, W) = \frac{2(\cos W - \cos H)}{H^2 - W^2}.$$

Step 1: Evaluate y_n'' and y_{n-1}''

From the fitting model,

$$y_n'' = -\lambda^2 y_n + g_n, \qquad y_{n-1}'' = -\lambda^2 y_{n-1} + g_{n-1}. \tag{106}$$

Step 2: Substitute the model into the predictor

Using the first relation in the acceleration identities in the predictor,

$$\begin{aligned} y_{n+1}^p &= 2y_n - y_{n-1} + ah^2(-\lambda^2 y_n + g_n) \\ &= (2 - aH^2)y_n - y_{n-1} + ah^2 g_n. \end{aligned} \tag{107}$$

Step 3: Evaluate the acceleration at the predicted point

The model equation is also used at x_{n+1}, with the predicted value in place of y_{n+1}:

$$(y_{n+1}^p)'' = -\lambda^2 y_{n+1}^p + g_{n+1}. \tag{108}$$

Substituting the predicted value gives

$$(y_{n+1}^p)'' = -\lambda^2(2 - aH^2)y_n + \lambda^2 y_{n-1} - aH^2 g_n + g_{n+1}. \tag{109}$$

Step 4: Form the symmetric acceleration combination

Add $(y_{n+1}^p)''$ and y_{n-1}''. From the acceleration identities and the predicted acceleration,

$$\begin{aligned} (y_{n+1}^p)'' + y_{n-1}'' = &-\lambda^2(2 - aH^2)y_n + \lambda^2 y_{n-1} - \lambda^2 y_{n-1} \\ &- aH^2 g_n + g_{n+1} + g_{n-1}. \end{aligned} \tag{110}$$

The two terms containing y_{n-1} cancel exactly. Hence

$$(y_{n+1}^p)'' + y_{n-1}'' = -\lambda^2(2 - aH^2)y_n + \left(2\cos W - aH^2\right) g_n. \tag{111}$$

This cancellation is the key algebraic simplification. It is the reason why the corrector can be reduced to a three-term recurrence with only y_{n+1}, y_n, y_{n-1}.

Step 5: Substitute into the corrector

Insert the symmetric acceleration identity and $y_n'' = -\lambda^2 y_n + g_n$ into the corrector:

$$\begin{aligned} y_{n+1} - 2y_n + y_{n-1} = &-H^2 \left[b_0(2 - aH^2) + b_1\right] y_n \\ &+ h^2 \left[b_0(2\cos W - aH^2) + b_1\right] g_n. \end{aligned} \tag{112}$$

Move the y_n-term to the left. The numerical method therefore satisfies the difference equation

$$\boxed{y_{n+1} - A(H, W)y_n + y_{n-1} = h^2 B(H, W)e^{\mathrm{i}\omega x_n}} \tag{113}$$

where

$$\boxed{A(H, W) = 2 - H^2 \left[b_0(2 - aH^2) + b_1\right]} \tag{114}$$

and

$$\boxed{B(H, W) = b_0(2\cos W - aH^2) + b_1.} \tag{115}$$

Equation the numerical difference equation is the requested three-term difference equation obtained directly by applying the model problem to the new numerical method.

Use of the Numerov normalization

The classical Numerov consistency condition is

$$\boxed{2b_0 + b_1 = 1.} \tag{116}$$

Thus

$$b_1 = 1 - 2b_0. \tag{117}$$

Step 6: Simplify the homogeneous coefficient

Substitution of the normalization relation into the homogeneous coefficient yields

$$\begin{aligned} A(H,W) &= 2 - H^2\left[b_0(2 - aH^2) + 1 - 2b_0\right] \\ &= 2 - H^2\left(1 - ab_0H^2\right). \end{aligned} \tag{118}$$

Therefore the left-hand side of the numerical recurrence is independent of W after normalization.

Step 7: Simplify the forcing coefficient

Likewise,

$$\begin{aligned} B(H,W) &= b_0(2\cos W - aH^2) + 1 - 2b_0 \\ &= 1 + 2b_0(\cos W - 1) - ab_0H^2 \\ &= 1 - 4b_0\sin^2\left(\frac{W}{2}\right) - ab_0H^2. \end{aligned} \tag{119}$$

Consequently, the normalized numerical difference equation is

$$\boxed{\begin{aligned} &y_{n+1} - \left[2 - H^2(1 - ab_0H^2)\right] y_n + y_{n-1} \\ &\qquad = h^2\left[1 - ab_0H^2 - 4b_0\sin^2\left(\frac{W}{2}\right)\right] e^{\mathrm{i}\omega x_n}. \end{aligned}} \tag{120}$$

Exact difference equation of the differential model

We now derive the exact grid recurrence satisfied by every exact solution of the fitting model.

Step 8: Solve the differential equation

For $\omega \neq \lambda$, the general solution is

$$y(x) = A_1 e^{\mathrm{i}\lambda x} + A_2 e^{-\mathrm{i}\lambda x} + \frac{e^{\mathrm{i}\omega x}}{\lambda^2 - \omega^2}. \tag{121}$$

Step 9: Apply the centered exact operator

Consider

$$\mathcal{L}_H[y_n] = y_{n+1} - 2\cos(H)y_n + y_{n-1}. \tag{122}$$

For the homogeneous modes,

$$\mathcal{L}_H[e^{\pm\mathrm{i}\lambda x_n}] = 0, \tag{123}$$

because

$$e^{\pm\mathrm{i}H} - 2\cos H + e^{\mp\mathrm{i}H} = 0.$$

For the forcing mode,

$$\begin{aligned} \mathcal{L}_H[e^{\mathrm{i}\omega x_n}] &= \left(e^{\mathrm{i}W} - 2\cos H + e^{-\mathrm{i}W}\right) e^{\mathrm{i}\omega x_n} \\ &= 2(\cos W - \cos H)e^{\mathrm{i}\omega x_n}. \end{aligned} \tag{124}$$

Using

$$\lambda^2 - \omega^2 = \frac{H^2 - W^2}{h^2},$$

the particular solution in the exact solution gives

$$\boxed{y_{n+1} - 2\cos(H)y_n + y_{n-1} = h^2\Phi(H,W)e^{\mathrm{i}\omega x_n}} \tag{125}$$

where

$$\boxed{\Phi(H,W) = \frac{2(\cos W - \cos H)}{H^2 - W^2}.} \tag{126}$$

Thus there are now two recurrences:

- the *numerical recurrence* (120), obtained by applying the model to the proposed method;
- the *exact recurrence* (125), obtained from the exact solution of the differential model.

The coefficient functions are obtained by equating the corresponding terms of the two recurrences.

Matching the two difference equations

Step 10: Match the homogeneous coefficient

Compare the coefficient of y_n in (120) and (125). Exact natural-frequency propagation requires

$$2 - H^2(1 - ab_0H^2) = 2\cos H. \tag{127}$$

Hence

$$H^2(1 - ab_0H^2) = 2(1 - \cos H). \tag{128}$$

Define

$$\boxed{S(H) = \frac{2(1-\cos H)}{H^2} = \left[\frac{\sin(H/2)}{H/2}\right]^2.} \tag{129}$$

Then

$$\boxed{1 - ab_0H^2 = S(H).} \tag{130}$$

Equivalently,

$$\boxed{ab_0 = \frac{1 - S(H)}{H^2}.} \tag{131}$$

Step 11: Match the forcing coefficient

The right-hand coefficient in (120) must equal the exact response factor $\Phi(H, W)$. Therefore

$$1 - ab_0H^2 - 4b_0\sin^2\left(\frac{W}{2}\right) = \Phi(H, W). \tag{132}$$

Using (130),

$$S(H) - 4b_0\sin^2\left(\frac{W}{2}\right) = \Phi(H, W). \tag{133}$$

Solving for b_0 gives

$$\boxed{b_0(H, W) = \frac{S(H) - \Phi(H, W)}{4\sin^2(W/2)}.} \tag{134}$$

Step 12: Determine b_1

From the Numerov normalization (116),

$$\boxed{b_1(H, W) = 1 - 2b_0(H, W).} \tag{135}$$

Step 13: Determine a

From (130),

$$aH^2b_0 = 1 - S(H), \tag{136}$$

and hence

$$\boxed{a(H, W) = \frac{1 - S(H)}{H^2b_0(H, W)}.} \tag{137}$$

Equations (134), (135), and (137) are exactly the coefficient formulas of the new two-frequency response-fitted Numerov-type method.

The connection in one chain of implications

The complete derivation may be summarized as

$$\boxed{\begin{array}{c} y'' = -\lambda^2 y + e^{\mathrm{i}\omega x} \\ \Downarrow \quad \text{substitution into predictor–corrector} \\ y_{n+1} - \left[2 - H^2(1 - ab_0H^2)\right] y_n + y_{n-1} \\ = h^2 \left[1 - ab_0H^2 - 4b_0 \sin^2(W/2)\right] e^{\mathrm{i}\omega x_n} \\ \Downarrow \quad \text{match with the exact grid recurrence} \\ y_{n+1} - 2\cos H\, y_n + y_{n-1} = h^2 \Phi(H,W) e^{\mathrm{i}\omega x_n} \\ \Downarrow \\ 1 - ab_0H^2 = S(H), \qquad S(H) - 4b_0 \sin^2(W/2) = \Phi(H,W), \\ 2b_0 + b_1 = 1 \\ \Downarrow \\ b_0 = \dfrac{S - \Phi}{4\sin^2(W/2)}, \qquad b_1 = 1 - 2b_0, \qquad a = \dfrac{1 - S}{H^2 b_0}. \end{array}} \tag{138}$$

This shows precisely how the three-term difference equation is the bridge between the differential fitting model and the closed-form coefficients of the new method.

Stable form and the diagonal case

The quotient in (126) should not be evaluated directly when H and W are close. Using

$$\cos W - \cos H = 2 \sin\left(\frac{H+W}{2}\right) \sin\left(\frac{H-W}{2}\right),$$

we obtain

$$\boxed{\Phi(H,W) = \operatorname{sinc}\left(\frac{H+W}{2}\right) \operatorname{sinc}\left(\frac{H-W}{2}\right), \qquad \operatorname{sinc} z = \frac{\sin z}{z}.} \tag{139}$$

Therefore, on the diagonal $W = H$,

$$\boxed{\Phi(H,H) = \frac{\sin H}{H}.} \tag{140}$$

The same formulas (134)–(137) then apply with this continuous value of Φ.

Classical limit

As $H, W \to 0$,

$$S(H) = 1 - \frac{H^2}{12} + O(H^4), \tag{141}$$

and expansion of $\Phi(H,W)$ in the coefficient formulas yields

$$\boxed{a \longrightarrow 1, \qquad b_0 \longrightarrow \frac{1}{12}, \qquad b_1 \longrightarrow \frac{5}{6}.} \tag{142}$$

Thus the fitted method is a continuous frequency-dependent extension of the classical Numerov-type predictor–corrector.

Completion of the proof of Theorem 1. By Lemmas 1 and 2, exact matching requires

$$1 - ab_0H^2 = S(H), \qquad S(H) - 4b_0 \sin^2(W/2) = \Phi(H,W), \qquad 2b_0 + b_1 = 1.$$

Solving these three relations gives exactly the coefficient formulas stated in Theorem 1. If $\sin(W/2) \neq 0$, the second relation fixes b_0 uniquely, after which the normalization fixes b_1 and the first relation fixes a. At $W = 2k\pi$ the sampled forcing is aliased and this identification degenerates. Finally, equality of the numerical and exact grid recurrences proves exactness on the three fitted grid modes when the starting values are exact. □

B. Proof of Theorem 2

Lemma 3 (Stable representation of the response factor)**.** *The response factor admits the representation*

$$\Phi(H,W)=\operatorname{sinc}\left(\frac{H+W}{2}\right)\operatorname{sinc}\left(\frac{H-W}{2}\right),\qquad \operatorname{sinc} z=\frac{\sin z}{z}.$$

Consequently $\Phi(H,H)=\sin H/H$*.*

Proof. Use $\cos W-\cos H=2\sin((H+W)/2)\sin((H-W)/2)$ and $H^2-W^2=(H+W)(H-W)$. The diagonal value follows by continuity of sinc at the origin. □

Proof of Theorem 2. Lemma 3 removes the apparent singularity at $W=H$ and may be inserted directly into the coefficient formulas of Theorem 1. Expanding $\sin z$ and $\cos z$ at the origin gives $S(H)=1-H^2/12+O(H^4)$ and the corresponding expansion of Φ. Substitution yields $b_0\to 1/12$, $b_1\to 5/6$, and $a\to 1$. Carrying the same formal series calculation through total degree ten gives the series displayed in Section 4. Substitution $W=H$ into the bivariate series produces term by term the independently expanded diagonal series; therefore their difference begins at $O(h^{12})$. □

C. Proof of Theorem 3

Proof. For $y''=-\mu^2 y$ the predictor is $y^p_{n+1}=(2-aV^2)y_n-y_{n-1}$. Substitution into the corrector and use of $2b_0+b_1=1$ give

$$A_s=1-\frac{V^2}{2}+\frac{ab_0}{2}V^4.$$

The homogeneous fitting relation in Theorem 1 gives $ab_0=(1-S(H))/H^2=c(H)$, so W disappears. The characteristic polynomial has product of roots equal to one. If $|A_s|<1$, its two roots are distinct complex conjugates and therefore both have unit modulus, proving periodicity and zero dissipation. Finally,

$$A_s(H;H)=1-\frac{H^2}{2}+\frac{1-S(H)}{2}H^2=1-\frac{H^2S(H)}{2}=\cos H.$$

□

D. Proof of Theorem 4 and Corollary 1

Lemma 4 (Predictor defect)**.** *For exact starting values and fixed* λ,ω*,*

$$y^p_{n+1}-y(x_{n+1})=-h^4\left[\frac{y^{(4)}(x_n)}{12}+\frac{\omega^2y''(x_n)}{20}\right]+O(h^5).$$

Proof. Insert the Taylor expansion of $y(x_{n-1})$ in the predictor and use the small-step expansion $a=1-\omega^2h^2/20+O(h^4)$. Cancellation of the terms through degree three gives the stated expression. □

Proof of Theorem 4. Expand the centered exact difference and both endpoint accelerations about x_n. In the predicted endpoint acceleration use

$$f(x_{n+1},y^p_{n+1})=f(x_{n+1},y(x_{n+1}))+f_y\big(y^p_{n+1}-y(x_{n+1})\big)+O(h^5),$$

together with Lemma 4 and the coefficient expansions of Section 4. Collecting the h^6 terms gives

$$\mathcal{T}^{\text{new}}_{n+1}=h^6\left[-\frac{1}{240}y^{(6)}+\left(\frac{f_y}{144}+\frac{\lambda^2}{360}-\frac{\omega^2}{240}\right)y^{(4)}+\frac{f_y\omega^2}{240}y''\right]_{x=x_n}+O(h^7).$$

Thus the unscaled defect is $O(h^6)$, establishing local algebraic order four. Global convergence follows under the additional assumptions of Appendix 11. For the fitted equation, Theorem 1 gives the stronger statement that the numerical and exact grid recurrences coincide, hence the fitted grid defect is identically zero. □

Proof of Corollary 1. For $y''=-\mu^2y$ use $f_y=-\mu^2$, $y^{(4)}=\mu^4y$, and $y^{(6)}=-\mu^6y$ in Theorem 4. Simplification gives

$$\mathcal{T}^{\text{new}}_{n+1}=\frac{\mu^4(\lambda^2-\mu^2)}{360}h^6y(x_n)+O(h^7),$$

which vanishes to leading order at $\mu=\lambda$. □

E. Implementation safeguards and reproducibility notes

For small H, $S(H)$ should be evaluated from its sinc form. Near the diagonal the response factor should be evaluated with Lemma 3, and near the origin the Taylor expansions of Section 4 should replace the raw quotients. When λ, ω, and h are constant, all fitted coefficients should be computed before the stepping loop. Numerical reports should state the arithmetic precision, starting procedure, error norm, timing protocol, and the precise published tableaux of all comparison methods.

References

1. P. J. van der Houwen, B. P. Sommeijer, K. Strehmel and R. Weiner, “On the numerical integration of second-order initial value problems with a periodic forcing function,” Computing 37 (1986), 195–218.

2. T. E. Simos and P. S. Williams, “New insights in the development of Numerov-type methods with minimal phase-lag for the numerical solution of the Schrödinger equation,” Computers & Chemistry 25 (2001), 77–82.

3. T. E. Simos, I. Th. Famelis and Ch. Tsitouras, “Zero dissipative, explicit Numerov-type methods for second order IVPs with oscillating solutions,” Numerical Algorithms 34 (2003), 27–40.

4. T. E. Simos and Ch. Tsitouras, “A new family of 7 stages, eighth-order explicit Numerov-type methods,” Mathematical Methods in the Applied Sciences 40 (2017), 7867–7878.

5. H. Van de Vyver, “An explicit Numerov-type method for second-order differential equations with oscillating solutions,” Computers & Mathematics with Applications 53 (2007), 1339–1348.

6. H. Van de Vyver, “Phase-fitted and amplification-fitted two-step hybrid methods for $y'' = f(x, y)$,” Journal of Computational and Applied Mathematics 209 (2007), 33–53.

7. Y. Fang, X. You and Z. Chen, “New phase fitted and amplification fitted Numerov-type methods for periodic IVPs with two frequencies,” Abstract and Applied Analysis (2012), Article ID 742585.

8. A. G. Bratsos, I. Th. Famelis, A. Kollias and Ch. Tsitouras, “Phase-fitted Numerov type methods,” Applied Mathematics and Computation 184 (2007), 23–29.

9. M. M. Chawla and P. S. Rao, “A Numerov-type method with minimal phase-lag for the integration of second order periodic initial value problems. II. Explicit method,” Journal of Computational and Applied Mathematics 15 (1986), 329–337.

10. J. R. Dormand and P. J. Prince, “A family of embedded Runge–Kutta formulae,” Journal of Computational and Applied Mathematics 6 (1980), 19–26.

11. J. R. Dormand, M. E. A. El-Mikkawy and P. J. Prince, “Families of Runge–Kutta–Nyström formulae,” IMA Journal of Numerical Analysis 7 (1987), 235–250.

12. J. R. Dormand, M. E. A. El-Mikkawy and P. J. Prince, “High-order embedded Runge–Kutta–Nyström formulae,” IMA Journal of Numerical Analysis 7 (1987), 423–430.

13. P. J. Prince and J. R. Dormand, “High order embedded Runge–Kutta formulae,” Journal of Computational and Applied Mathematics 7 (1981), 67–75.

14. E. Fehlberg, “Low-order classical Runge–Kutta formulas with stepsize control and their application to some heat transfer problems,” NASA Technical Report R-315, 1969.

15. E. Fehlberg, “Classical eighth- and lower-order Runge–Kutta–Nyström formulas with a new stepsize control procedure for special second-order differential equations,” NASA Technical Report R-410, 1973.

16. E. Fehlberg, “Neue Runge–Kutta–Nyström Formelpaare 3(4)-ter und 4(5)-ter Ordnung,” ZAMM 67 (1987), 367–372.

17. L. Gr. Ixaru and G. Vanden Berghe, *Exponential Fitting*, Mathematics and Its Applications, Vol. 568, Kluwer Academic Publishers, Dordrecht, 2004.

18. C. Lunk and B. Simeon, “Runge–Kutta–Nyström methods with maximized stability domain in structural dynamics,” Applied Numerical Mathematics 53 (2005), 373–389.

19. F. F. Ngwane, “A trigonometrically fitted block method for solving oscillatory second-order initial value problems and Hamiltonian systems,” International Journal of Differential Equations (2017), Article ID 9293530.